An Adaptive Method of Symmetrical Component Estimation

R. Naidoo[1], P. Pillay[2], J. Visser[3], R. C. Bansal[1], and N. T. Mbungu[1]

[1]Dept. of Electrical, Electronics, and Computer Systems Engineering, University of Pretoria Hatfield, Pretoria 0028, South Africa, emails: raj.naidoo@up.ac.za, rcbansal@ieee.org, mbungunsilulu@gmail.com

[2]Department of Electrical and Computer Engineering, Montréal, Québec, Canada pillay@encs.concordia.ca

[3]AngloAmerican, Mpumalanga South Africa, jaco.visser@angloamerican.com

Highlights

- A new strategy of symmetrical component estimation is proposed.
- The extraction of the harmonic and noise levels on the system signal is developed.
- A Discrete Fourier Transform and an online algorithm to analyse the system performance are developed.
- A method to manage the amplitude change for system component in real-time is proposed.

Abstract

This paper proposes a smart approach of estimating the symmetrical component into a network. The Smart grid development and deployment offers serval advantages regarding the overall system performance of the electrical system. Currently, through the smart metering system, the symmetrical components problems can be resolved in real-time by extracting, tracking and detecting any issue related to power disturbance on the grid. An adaptive method to estimate symmetrical components in the framework of the smart grid is presented. The proposed method is based on a nonlinear adaptive tracking of amplitude, phase and frequency of a non-stationary sinusoidal waveform in real-time. The method offers structural simplicity while maintaining performance robustness and controllable speed and accuracy. Experimental results are presented to verify the performance of the proposed method. The results show that the method can provide an accurate estimation of the symmetrical components in the presence of amplitude and phase variations, as well as in the presence of harmonics. The simplicity of the structure and ease of the parameter settings render the proposed method suitable for both software and hardware implementation. Two scenarios are analysed to validate the proposed algorithm.

Index Terms—Symmetrical components, nonlinear filter, voltage tracking, real-time estimation.

1. Introduction

The topic of symmetrical components is standard in most textbooks on electrical power systems. A system that is considered balanced has three voltage and current signals that have equal magnitudes and 120° phase-displacements. When these conditions are not met, the system is unbalanced. The theory of symmetrical components indicates that an unbalanced set of signals can be decomposed into three balanced sets of signals. Symmetrical components find applications in a variety of power system problems such as protection, fault analysis, reactive power compensation, unbalance mitigation, and distributed generation. Many papers describe the application of symmetrical components [1]-[5]. Fortescue [6] introduced the theory of symmetrical components for complex phasors that can be applied to the solution of polyphase networks. Several methods of estimating symmetrical components have been proposed [7]-[19].

In [7], the smart power grid synchronization uses the effectiveness of real-time estimation into a novel nonlinear strategy to track the system frequency, voltage magnitudes and phase angles. This method employs the symmetrical component transformation separately, i.e. the positive, negative and zero sequences are analysed independently to be transformed into the stationary coordinate frame. This approach describes the system modelling, which contains a fault tolerant extended Kalman filter. In [8], the synchronization of unbalanced three-phase voltages with nonlinear estimation is performed through an extended Kalman filter and the unscented Kalman filter in the framework of the smart grid. This strategy uses the methodology of the symmetrical component transformation to apply Clarke's transformation that can describe the state space equation. The procedure aims to estimate the voltage magnitude and phase angle. In [9], an adaptive notch filtering method based synchronization technique is introduced. This is a modified structure where the three-phase quantities are decomposed into symmetrical components, harmonics are extracted, the frequency variation is tracked, and the voltage regulation and reactive power control are provided. The proposed strategy has an advantage of do not require a phase-locked loop for the synchronisation. In [10], a pre-filter based phase locked loop for three-phase grid-connected applications is proposed. This approach is fast and precise regarding phase estimation for both unbalanced and high distorted three-phase electric variables, and it can control the system equipment and dynamic voltage restorer.

Luna et al. in [11] propose an algorithm for phase angle estimation based on symmetrical sequence components. This strategy applies the recursive weighted least-squares structure that can estimate the negative and positive sequences. It is observed that the proposed approach is capable of eliminating the low order harmonics and direct current offset in the sampled variables. In [12], a new state-space model in the framework of the extended Kalman filter that can estimate the symmetrical components of distorted and time changing power systems is introduced. This model can detect and quantify the overall three-phase power system unbalance problem, and the algorithm has the capability of deducing in each interaction the amplitudes and phase angle values of the symmetrical components. In [13], a novel fast detection algorithm for grid symmetrical components extraction is proposed. This new generation algorithm utilises the complex least squares strategy. This method applies a quick and accurate detection of the amplitude and phase of grid voltage for both the positive and negative sequence when the system voltage has high order harmonics and random noise. In 1992 Pinto de Sá [14] has introduced a new Kalman filter approach that supports symmetrical components based distance estimator with moderate sampling rate for digital relaying. The paper describes how to include the Kalman filter state space analogic pre-filters' transients simply. It also presents how to handle the colouring effect of the pre-filters and the network into the model.

The Discrete Fourier Transform (DFT) is proposed as one of the algorithm methods that can be easily embedded in hardware for power system real-time phasor estimations [15]. Carugati et al. [16] have presented a new method of measuring the three-phase harmonic and sequence components by using a sliding DFT and variable sampling period technique. This strategy also permits the computation of the corresponding imbalance by guessing the instantaneous symmetrical components. In [17], a modified artificial bee colony algorithm method is proposed to estimate the solution of the power system harmonic. This approach can provide excellent basic designing active filters that can be exploited in power system. The Kalman Filter, as a recursive estimator, is introduced as a powerful tool for the estimation of time-varying parameters of symmetrical components. The filter has the capability of processing noisy measurements, and it gives a least a square optimal estimate. The main drawback of the Kalman Filter is the number of calculations that it must perform. Kusljevic [18] proposed the use of the Enhanced Phase-Locked Loop for symmetrical component estimation. This method takes longer than a cycle to provide its response but can provide an accurate estimate when power frequency excursions occur. A non-recursive Newton-type numerical algorithm is presented in [19]. This approach is used with the second stage algorithm for symmetrical

components calculation that derives from the estimated fundamental phasors of the arbitrary voltages or currents in three-phase system signals.

The algorithm has linearity, is very simple, and involves moderate computation. The Newton-type algorithm provides accuracy and is not sensitive to power-system frequency deviations and harmonic distortions in three-phase signals. The different approaches include stochastic estimation theory, Kalman filters, weighted least-squares estimations, and time-domain methods. In most papers presented, there has been much argument presented with little focus on the practical application [5], [7] - [20]. However, some practical applications in the framework of a smart grid have been developed in conjunction with network synchronisation of fault-tolerant estimation and renewable energy integration [21]. Thus, the influence of frequency deviations, harmonics and noise can affect the performance of the different methods. This has also received little attention in real-time estimation strategy. The proposed method is based on converting the input signal into phasors. This is done by an estimation of the magnitude, phase angle, and frequency of an input signal. From this, the sequence components are computed in the time-domain. An overview of the approach is shown in Figure 1.

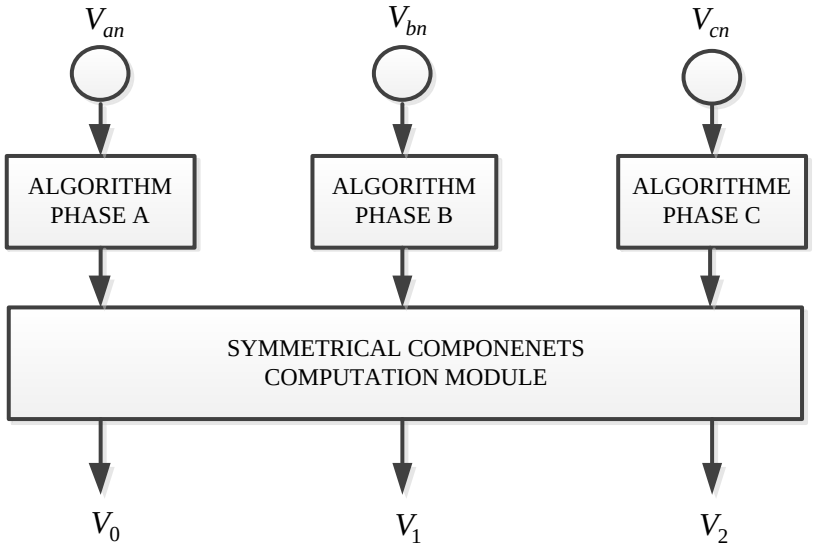

Fig 1: Overview of the proposed approach.

The main contribution of this proposed approach is to develop a DFT and an online algorithm that can analyse the system performance through an adaptive method of symmetrical component estimation. This study is simulated in Matlab Simulink, and an experimental study is investigated by using an Omicron 56 and a TMS320F240 processor. Both scenarios aim to contribute in these following points as:

1. Develop a method that can handle the amplitude changes on the electrical system in real time for better control of the network

2. Propose a new strategy of symmetrical component estimation in real-time that can tract any change into the phase angle by using a DFT and algorithm.
3. Develop a dynamic approach to extract the harmonic and noise levels on the system signal.

The paper is organized as follows: Section 2 presents a description of the adaptive algorithm. An adaptive model of the symmetrical component estimation is described in Section 3. The simulation performance under the influence of step changes in amplitude and phase, as well as, the influence of harmonics and noise is presented in Section 4. The experimental testing of the formulated model is shown in Section 5. In Section 6, actual faulted data is used to evaluate the proposed method, and Section 7 presents the conclusion of the paper.

2. Formulation of the Non-Linear Filter

The adaptive symmetrical component estimation model is formulated based on the nonlinear adaptive filter of Ziarani and Konrad [22]. Let *v(t)* represents a voltage signal in which *n(t)* denotes the superimposed disturbance or noise. In atypical operation i.e. a power system, *v(t)* has a general form of:

$$v(t) = \sum_{i=0}^{\infty} V_i \sin(\omega t + \phi) + n(t) \tag{1}$$

where V is the system voltage, ω is the angular frequency and ϕ is the phase angle. All these parameters, V, ω and ϕ, are functions of time. In a power system, this function is usually continuous and almost periodic. A sinusoidal component of this function is:

$$S(t) = V_s \sin(\omega t + \delta_s) \tag{2}$$

where V_s is the amplitude, ω the frequency and δ_s the phase angle. These parameters vary with time depending on the load, as well as the occurrence of faults in the power system. The adaptive algorithm presented, extracts a specified component of *v(t).* Let M be a manifold containing all sinusoidal signals defined as:

$$M = \{V(t)\sin(\omega(t)t + \delta(t))\} \tag{3}$$

where:

$$\begin{aligned} &V(t) \in [V_{\min}, V_{\max}], \\ &\omega(t) \in [\omega_{\min}, \omega_{\max}], \\ &\delta(t) \in [\delta_{\max}, \delta_{\min}] \end{aligned} \tag{4}$$

Thus:

$$\Im(t) = \left[V(t), \omega(t), \delta(t)\right]^T \tag{5}$$

With $\Im(t)$ as a vector of the parameters which belongs to the parameter space:

$$\vartheta = \left[V, \omega, \delta\right]^T \tag{6}$$

It is important to note that, *T* denotes the transposition matrix. The output is defined as the desired sinusoidal component:

$$S(t, \Im(t)) = V(t)\sin(\omega(t)t + \delta(t)) \tag{7}$$

In order to extract a certain sinusoidal component of *v(t)*, the solution has to be an orthogonal projection of *v(t)* onto the manifold *M*. Alternatively it has to be an optimum ϕ that minimizes the distance function *d* between $y(t, \theta(t))$ and *v(t)* i.e.:

$$\Im_{opt} = \arg \min_{\Im(t) \in \vartheta} d\left[s(t, \Im(t)), v(t)\right] \tag{8}$$

Without being concerned about the mathematical correctness of the definition of least squared error, which strictly speaking has to continue onto the set of real numbers. The instantaneous distance function *d* is used:

$$d^2(t, \zeta(t)) = \left[v(t) - s(t, \Im(t)\right]^2 \underline{\underline{\Delta}} e(t)^2 \tag{9}$$

The cost function is defined as:

$$J(\zeta(t), t) \underline{\underline{\Delta}} d^2(t, \zeta(t)) \tag{10}$$

Although the cost function is not quadratic, the parameter vector $\Im$ is estimated using the quadratic decent method:

$$\frac{d\Im(t)}{dt} = \mu \frac{\partial\left[J(t, \Im(t)\right]}{\partial \Im(t)} \tag{11}$$

The estimated parameter vector is thus denoted by:

$$\hat{\Im}(t) = \left[\hat{V}(t), \hat{\omega}(t), \hat{\delta}(t)\right]^T \tag{12}$$

The complete mathematical proof is presented in [11]. The governing set of equations of the adaptive algorithm is:

$$\dot{V} = k_1 e \sin\phi \tag{13}$$

$$\dot{\omega} = k_2 eV \cos\phi \tag{14}$$

$$\dot{\phi} = k_3 eA \cos\phi + \omega \tag{15}$$

$$s(t) = V \sin\phi \tag{16}$$

$$e(t) = v(t) - s(t) \tag{17}$$

where *v(t)* and *s(t)* are the respective input and output signals of the core algorithm. The dot represents the differentiation with respect to time and the error signal *e(t)* is *v(t) – s(t)*. The state variables *V*, *f* and ω directly provide estimates of the amplitude, phase, and frequency of *v(t)*. Parameters k_1, k_2, and k_3 are positive numbers that determine the behaviour of the algorithm in terms of convergence speed and accuracy. Parameter k_1 controls the speed of the transient response of the algorithm with respect to the variations in the amplitude of the interfering signal. Parameters k_1 and k_3 control the speed of the transient response of the algorithm with respect to variations in the frequency of the interfering signal. The dynamics of the algorithm presents a notch filter in the sense that it extracts a specific sinusoidal component and rejects all the other components including noise. The centre frequency of such an adaptive notch filter is specified by the initial condition of frequency ω [23]. It is in the form of the composition of simple blocks suitable for schematic software development tools. A graphical representation is shown in Figure 2.

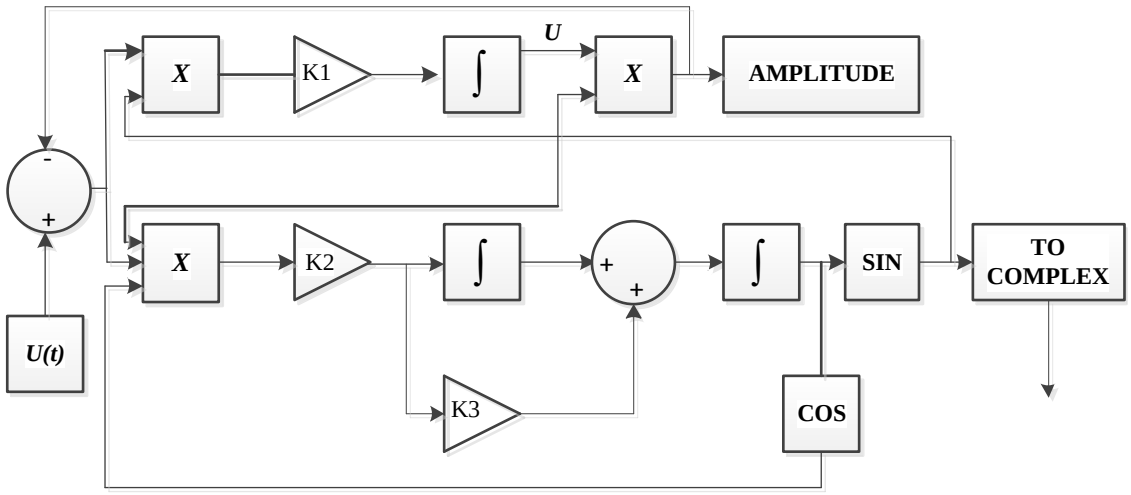

Fig. 2. Conversion of time domain input signal into a phasor.

3. Symmetrical Component Adaptive Model

Consider the three-phase set of symmetrical signals represented by (18) as follows:

$$U = \begin{bmatrix} u_a \\ u_b \\ u_c \end{bmatrix} = \begin{bmatrix} U_a(t)\sqrt{2}\cos(\omega t + \alpha_a(t)) \\ U_b(t)\sqrt{2}\cos(\omega t + \alpha_b(t)) \\ U_c(t)\sqrt{2}\cos(\omega t + \alpha_c(t)) \end{bmatrix} \tag{18}$$

where *u* denotes the instantaneous magnitude, *U(t)* the time varying peak amplitude of the waveform, and $\alpha(t)$ *is* the time varying phase of the waveform. Equation (18) can be written as the sum of two complex conjugated terms:

$$U = \frac{1}{\sqrt{2}} \begin{bmatrix} \underline{U_a} e^{j\omega t} + \underline{U_a^*} e^{-j\omega t} \\ \underline{U_b} e^{j\omega t} + \underline{U_b^*} e^{-j\omega t} \\ \underline{U_c} e^{j\omega t} + \underline{U_c^*} e^{-j\omega t} \end{bmatrix} \tag{19}$$

with

$$\begin{bmatrix} \underline{U_a} \\ \underline{U_b} \\ \underline{U_c} \end{bmatrix} = \begin{bmatrix} U_a(t) e^{j\alpha_a(t)} \\ U_b(t) e^{j\alpha_b(t)} \\ U_c(t) e^{j\alpha_c(t)} \end{bmatrix} \tag{20}$$

$\underline{U}$ denotes the phasor *u* and is determined by the estimating the amplitude *U(t)* and phase $\alpha(t)$ in (20). The proposed system for estimating these parameters is shown in Figure 3. The system in Figure 2 converts the time domain input signal into a phasor. The phasors are then converted into time domain symmetrical components as shown in Figure 3.

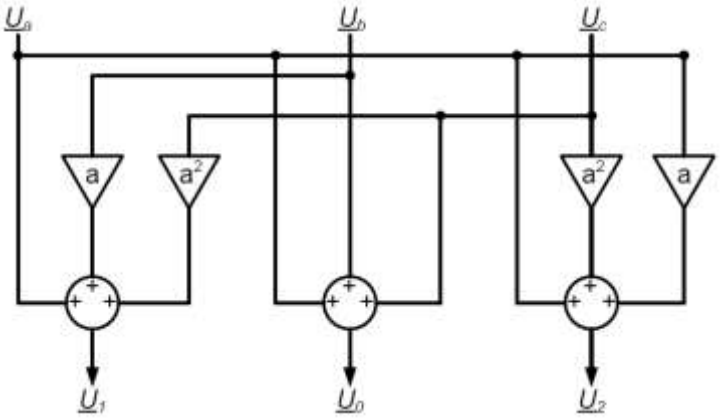

Fig. 3. Conversion of phasor components to symmetrical components.

The symmetrical component transformation matrix is described as

$$S = \begin{bmatrix} 1 & 1 & 1 \\ 1 & a & a^2 \\ 1 & a^2 & a \end{bmatrix}, \text{ where } \qquad a = e^{j\frac{2\pi}{3}} \tag{21}$$

Transformation into the symmetrical components time-domain $U = S^{-1}U$ yields [13]:

$$U = \begin{bmatrix} u^0 \\ u^1 \\ u^2 \end{bmatrix} = \frac{1}{\sqrt{2}} \begin{bmatrix} \underline{U_0} e^{j\omega t} + \underline{U_0^*} e^{-j\omega t} \\ \underline{U_1} e^{j\omega t} + \underline{U_0^*} e^{-j\omega t} \\ \underline{U_1} e^{j\omega t} + \underline{U_0^*} e^{-j\omega t} \end{bmatrix} \quad (22)$$

4. Performance of Proposed Method Through Simulation

This section investigates the performance of the proposed system by means of computer simulations. The following cases are studied:

- Case 1: Symmetrical component estimation for step changes in amplitude;
- Case 2: Symmetrical component estimation for step changes in phase; and
- Case 3: Symmetrical component estimation in signals with noise and harmonics.

For each case, the sequence components are theoretically calculated. This is used as a benchmark to compare the performance against the Discrete Fourier Transform (DFT). Performance comparisons are made in terms of speed of response and steady-state accuracy.

4.1. Effects of Change in Amplitude

Figure 4 shows the three-phase nominal input voltages of 230V (325 peaks) with a voltage dip of 0.4 pu from t = 0.4 to 0.8 seconds. This is typical of a sag in industry. The input voltages are V_a = 1∠0° pu, V_b = 1∠-120° pu and V_c =1∠120° pu. Theoretical calculated sequence components (in terms of the L-N peak) from Figure 5 are V_0 = 43.3V, V_1 = 282V and V_2 = 43.3V.

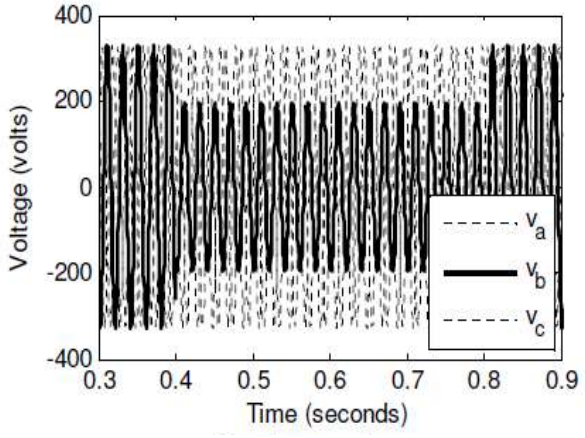

Fig. 4. Input waveform.

Figure 5 shows a comparison of the response of the adaptive algorithm and the Fourier sequence analyzers to a step change in amplitude. It is clear that the algorithm responds faster to a change in amplitude when compared to the Fourier method. A response time difference of

5 ms between the Fourier and proposed method was measured. The maximum steady-state error of the DFT and the proposed method are both 0.35%.

4.2. Effects of Change in Phase

The phase angle of Phase B is stepped by 30 ^{o} at t = 0.4 to 0.8 seconds. The input voltages are V_a = 325∠0^{o}, V_b = 325∠-90^{o} and V_c = 325∠120^{o}. Theoretical calculated sequence components are V_0 = 56.1∠-15^{o} V, V_1 = 315∠9.9^{o} V and V_2 = 56.1∠-135^{o} V. Figures 6 show the response of both methods to a step change in phase. The results show the steady-state error of both methods to be within 0.5%, and the non-linear filter responding 10ms quicker to the change in phase as compared to the DFT.

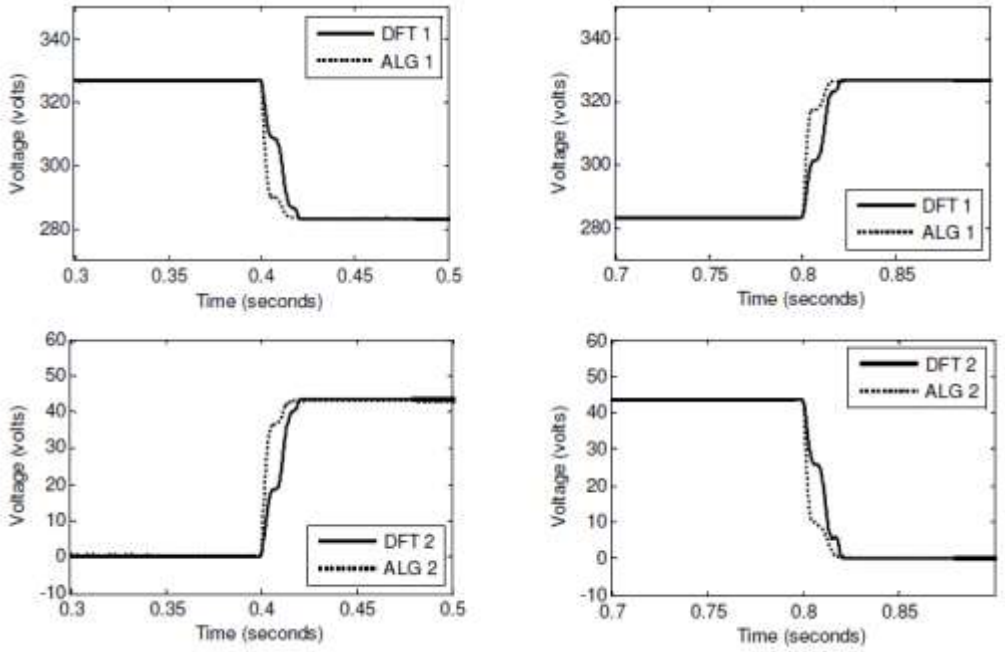

Fig. 5. Positive and negative sequence extraction (with change in Amplitude).

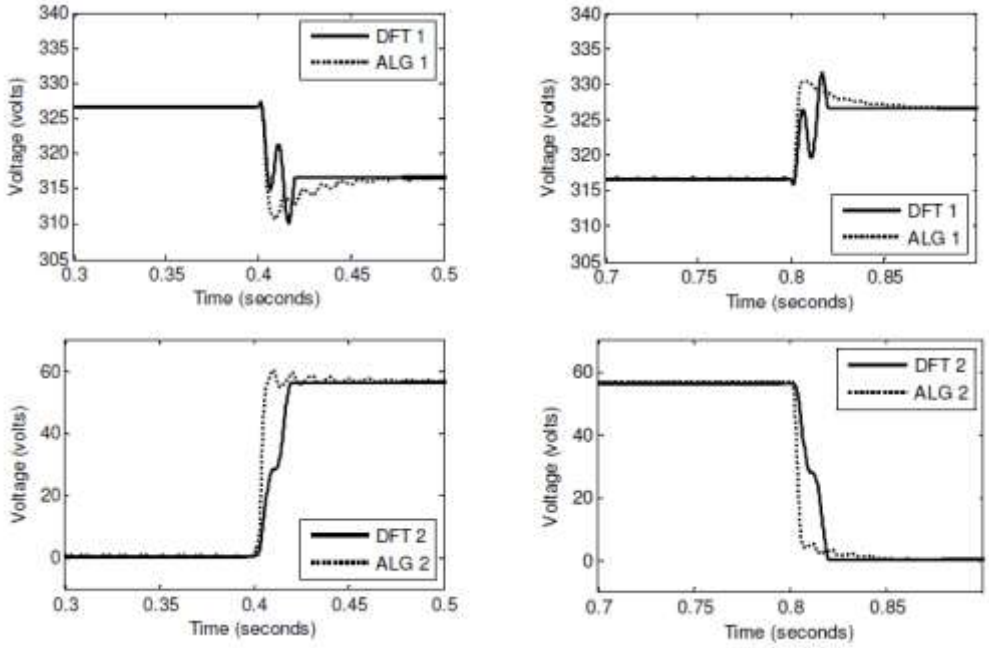

Fig. 6. Positive and negative sequence extraction (with change in phase).

4.3. Influence of harmonics and noise.

The performance of the algorithm and the DFT models in the presence of harmonic waveforms are shown in this section. Figure 7 (a) shows the input signal with peak amplitudes of 1.0 pu, 0.6 pu, and 1 pu for phase a, b and c respectively. The input signal is corrupted with a Gaussian noise with a zero mean and a variance of σ2 for which σ2 = 0.01 and SNR = 17 db. The DFT is capable of extracting the fundamental component under harmonic conditions. When the frequency of the harmonic is not an exact integer multiple, this poses a problem for the DFT. A 4.5th inter-harmonic of 10% magnitude is added to the waveform. Figures 7 (b) – (d) show a comparison between the response of the DFT and the proposed method of extracting the sequence components of the signal. Errors of 1.4%, 12.5% and 3% were obtained by using the DFT to extract the positive, negative and zero sequence voltages. The errors of the proposed method were 0.35%, 4%, and 3.5%. The results show that the influence of noise does influence the accuracy. For higher noise levels the nonlinear filter offers improved accuracy over the DFT.

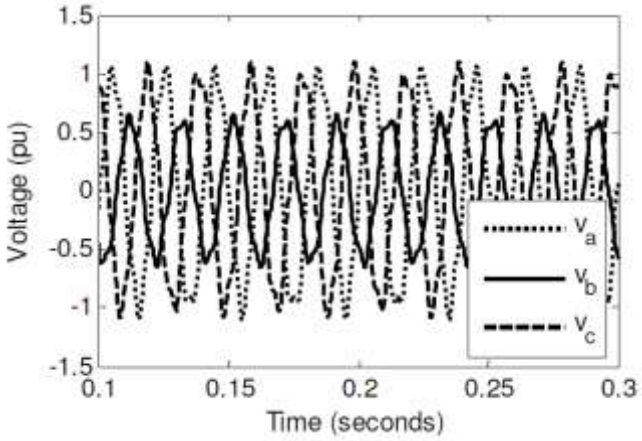

Fig. 7(a). Input waveform.

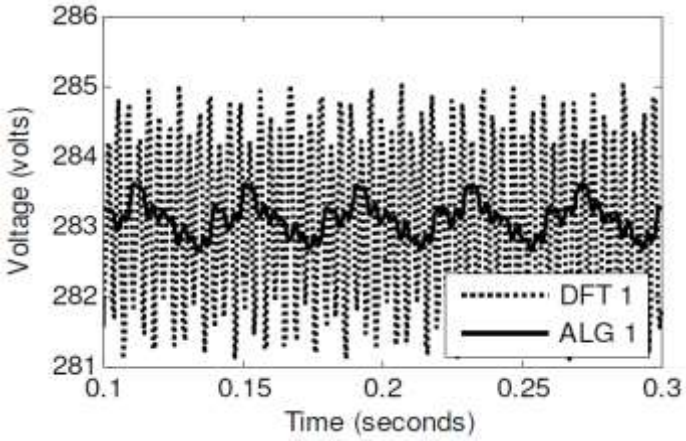

Fig. 7 (b). Positive sequence extraction.

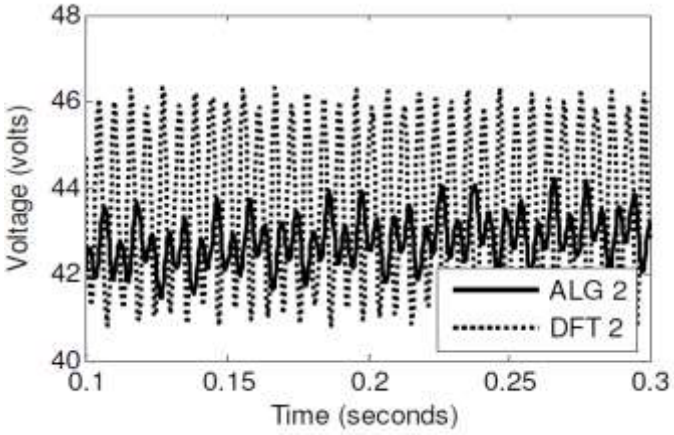

Fig. 7 (c). Negative sequence extraction.

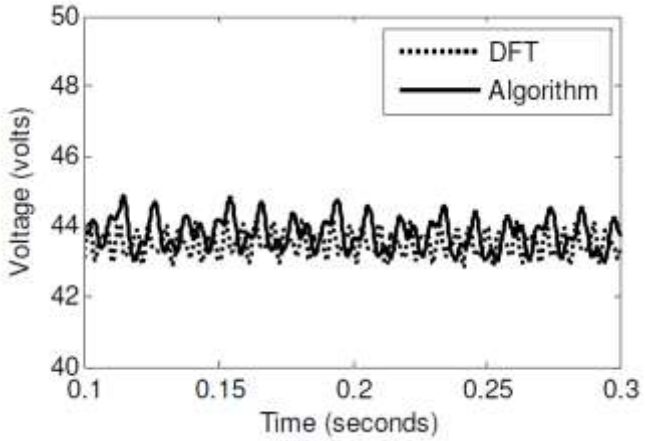

Fig. 7 (d). Zero sequence extraction.

5. Performance of Proposed Method Through Experimental Studies

Figure 8 shows the experimental setup that was arranged to conduct the experiments. An Omicron 56 three-phase injection set was used for this. A TMS320F240 processor was used to convert the analog signals from the Omicron 56 into digital signals that are input into the PC Operator.

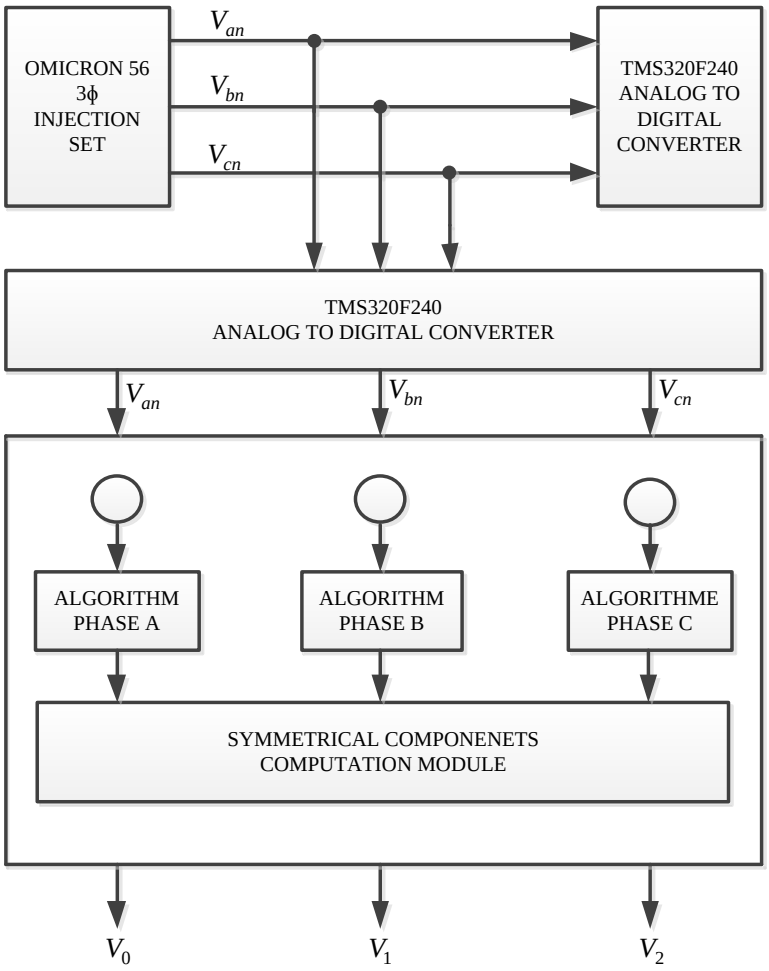

Fig. 8. Experimental setup for algorithm testing.

5.1. Effects of Change in Amplitude

Three-phase nominal input voltages of 110V (155.56 peak) with a 0.4 pu reduced voltage from t = 1 to 2 seconds were injected using the Omicron. The input voltages were: V_a =1∠0°, V_b = 0.4∠-120° and V_c = 1∠120°. Figure 9 shows a comparison for the positive, negative and zero sequence components of the response of the adaptive algorithm and the Fourier sequence analyser's system to a step change in amplitude. The algorithm responds faster to a change in amplitude as compared to the Fourier method. A maximum response time difference of 13ms between the Fourier and proposed method was obtained. The steady-state error was less than 1% for both methods. The effect of a 1pu/s ramp in the amplitude of Phase B is shown in Figure 10. This shows the resultant positive, negative and zero sequence components. For the positive sequence component results, both methods have an error less than 1%, while for the negative and zero sequence components the algorithm has an error of 1.2%. The DFT's error is less than 1%.

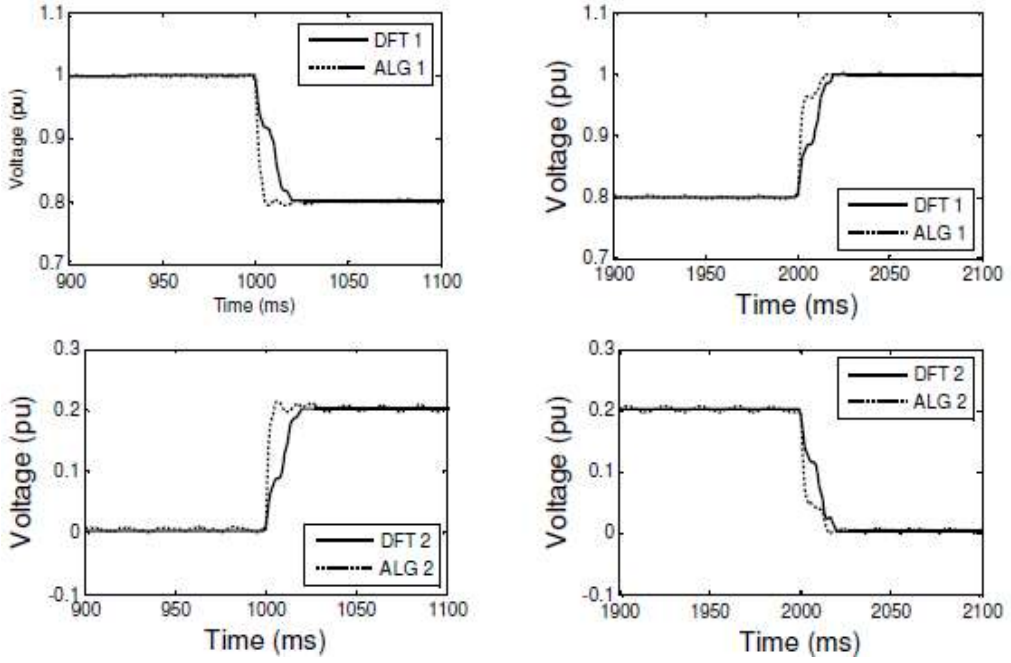

Fig. 9. Positive and negative sequence extraction.

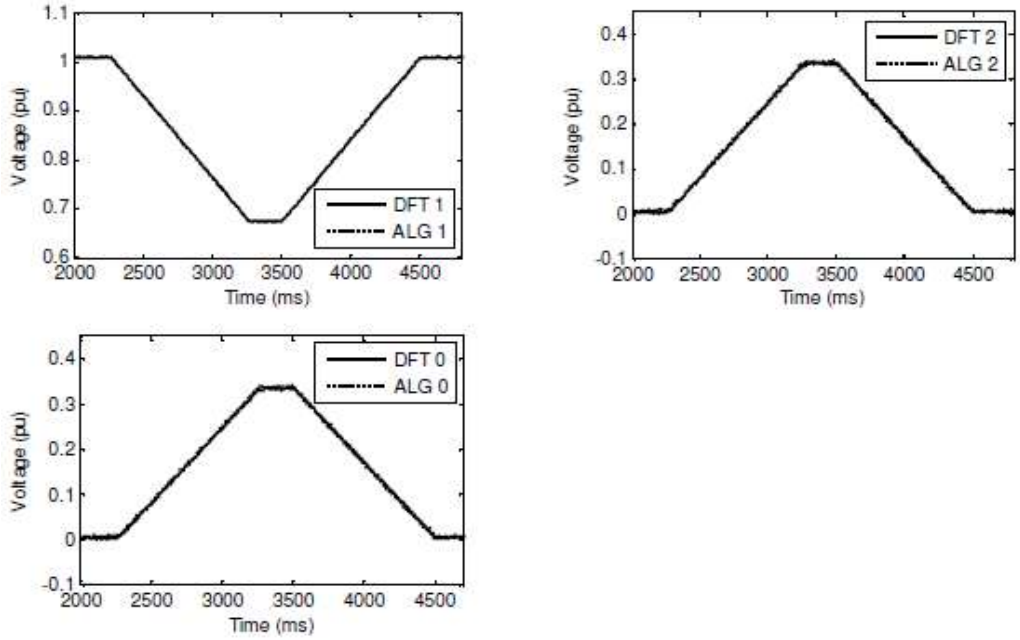

Fig. 10. Positive, negative and zero sequence extraction for a ramp in Amplitude.

5.2. Effects of Change in Phase

The phase angle of Phase B was stepped by 60° at t = 1 to 2 seconds. The input voltages are: $V_a = 1\angle 0°$, $V_b = 1\angle -60°$ and $V_c = 1\angle 120°$. Figure 11 shows the response of both methods to a step change in phase. The results show that the steady-state error of both methods for the positive and negative sequence components is less than 1%. The steady state error for the zero sequence of the DFT is less than 1%. The adaptive method has an error of 2%. The maximum

time response was measured. The algorithm responded 10.92ms faster than the DFT. The effect of an 80°/s ramp in the phase angle of Phase B is shown in Figure 12. This shows the resultant positive, negative and zero sequence components. For the positive sequence component estimation, both methods have an error of less than 1%. For the negative and zero sequence component estimation the algorithm has an error of 1.2% and the DFT's error is less than 1%.

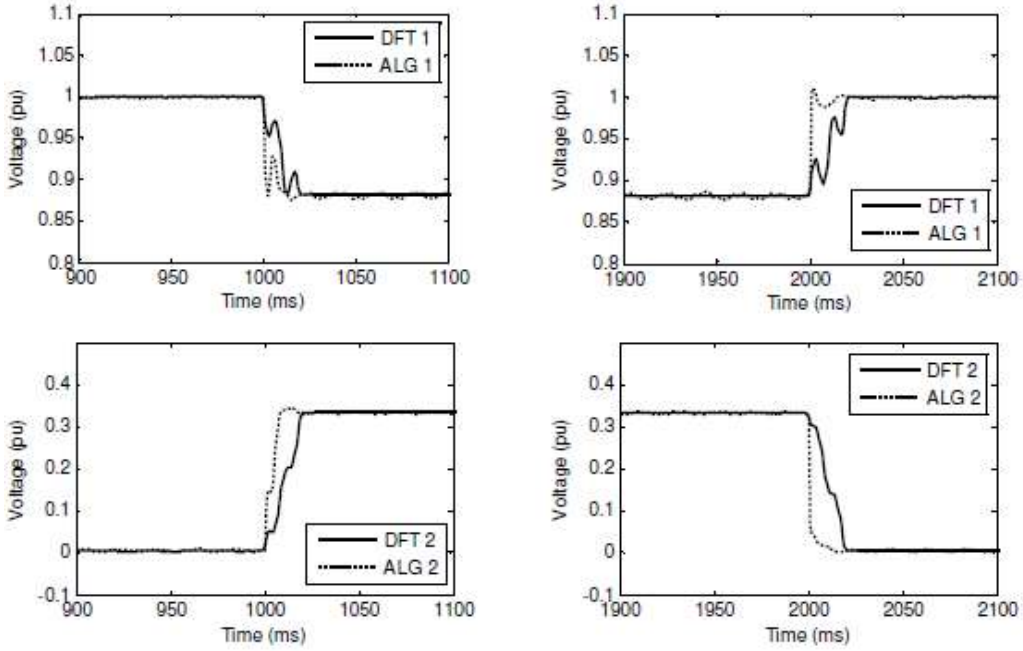

Fig. 11. Positive and negative sequence extraction.

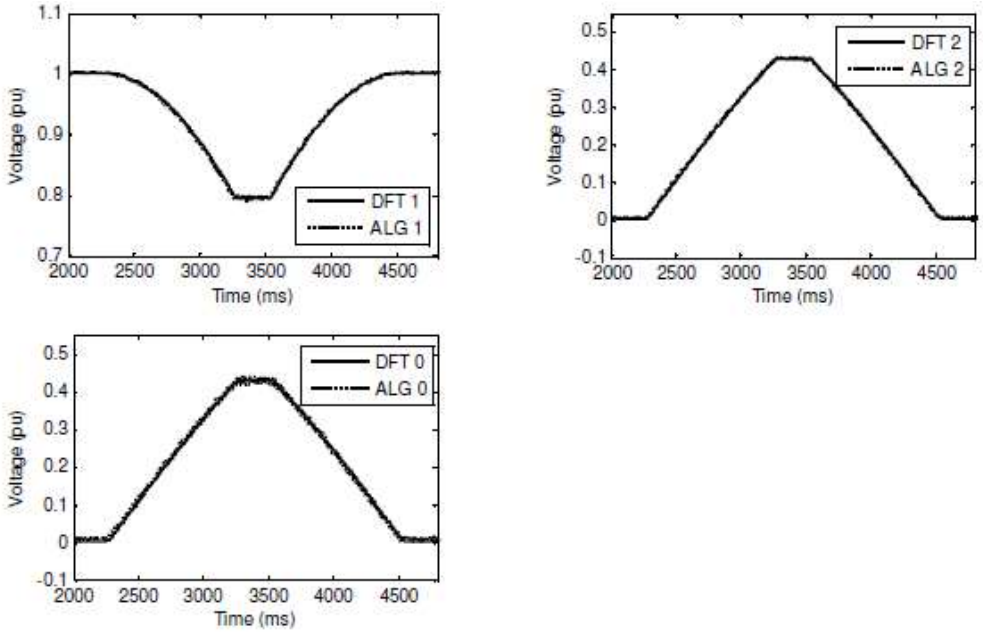

Fig. 12. Positive, negative and zero sequence extraction for a ramp in the phase angle.

5.3. Influence of harmonics and noise.

The performance of the algorithm and DFT models are demonstrated in this section with regard to harmonic noise. The amplitudes of the input signal with peak amplitudes are V_a = 1∠0°, V_b = 1∠-60° and V_c = 1∠120° for phase a, b and c respectively. A 4.5th inter-harmonic of 0.1pu is added to the input waveform. The harmonic waveform was built in Matlab and exported as a Comma Delimited Excel (CSV) file. A signal processing software package was then used to import the +CSV file in the format of a PQDIF file from where the software created an IEEE comtrade file. The comtrade file was then injected using the Omicron. Figure 13 (a) shows the input waveform. Performance of both methods with regard to harmonic noise on the input signal is very close, with steady state errors of less than 3% recorded for both models. The DFT has a more accurate zero-sequence component extraction. Figure 13 (b) – (d) show the positive, negative and zero sequence component results.

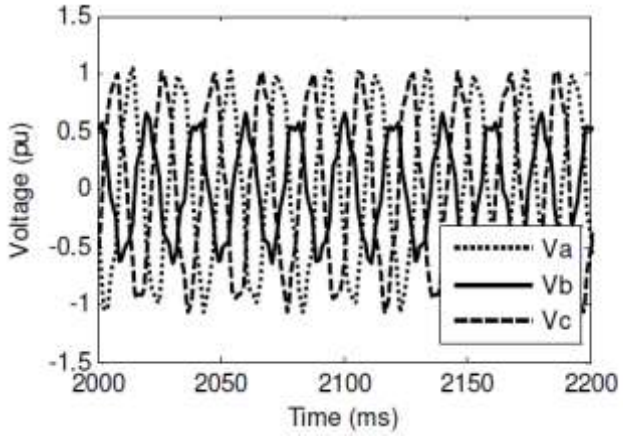

Fig. 13 (a). Input waveform.

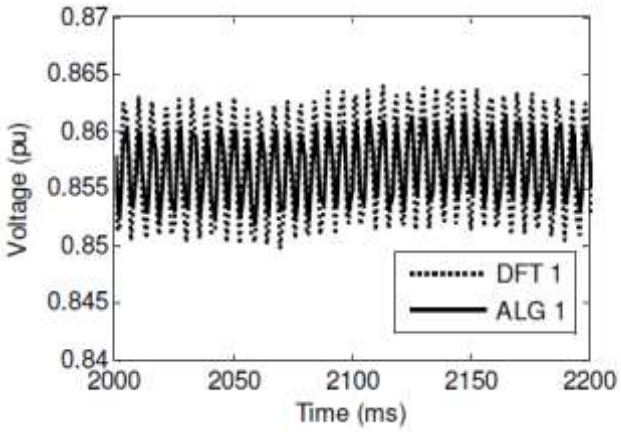

Fig. 13 (b). Positive sequence extraction.

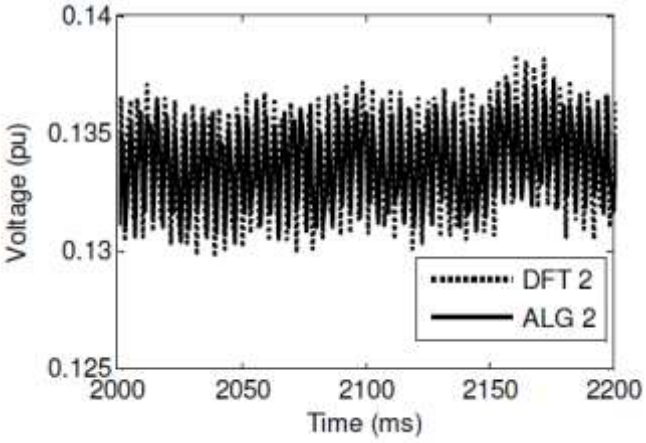

Fig. 13 (c). Negative sequence extraction.

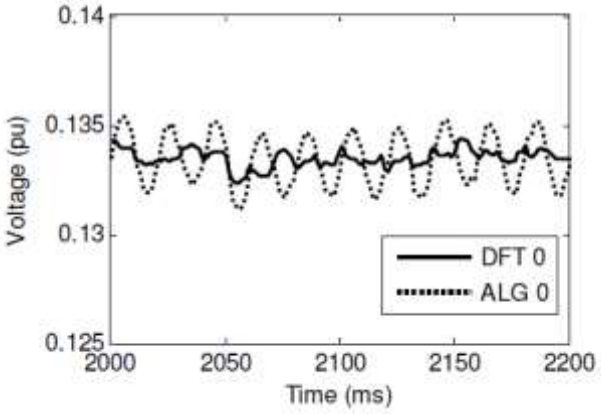

Fig. 13 (d). Zero sequence extraction.

6. *Application to Field Data*

Two different cases of transmission system fault types were studied. The DFT was used to benchmark the algorithm for the application to field data. Figure 14 shows the network where the fault occurred.

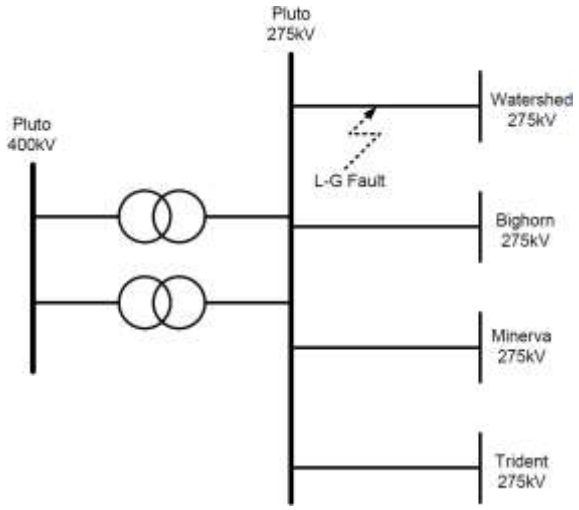

Fig. 14. Single line diagram for fault in case 2.

The protection relays captured and stored the fault in IEEE comtrade files. For the fault recreation, the Omicron injection set was used.

6.1. Case1

Fault Type 1 is a single line-ground fault on a 400 kV feeder. The source of the fault was a bird. The sampling frequency was 2.5 kHz. The pre/post-fault voltages are shown in Figure 15 (a). The fault occurred on Phase B at approximately 1.3 seconds. The results indicate that the non-linear algorithm model is able to track the symmetrical components of the voltage within 1% of the DFT on the positive sequence. The algorithm had a steady-state error of 4% in relation to that of the DFT on the negative and zero sequence components. The response of the algorithm model, at the inception of the fault, is 11.82 ms for the positive sequence and 14 ms for the negative and zero sequence components. The algorithm is able to respond faster than the DFT with acceptable accuracy. For the negative and zero sequences, the algorithm responds faster but with less accuracy than the DFT. Figures 15 (b) – (d) show a comparison of the algorithm and the DFT model for the positive, negative and zero sequence components.

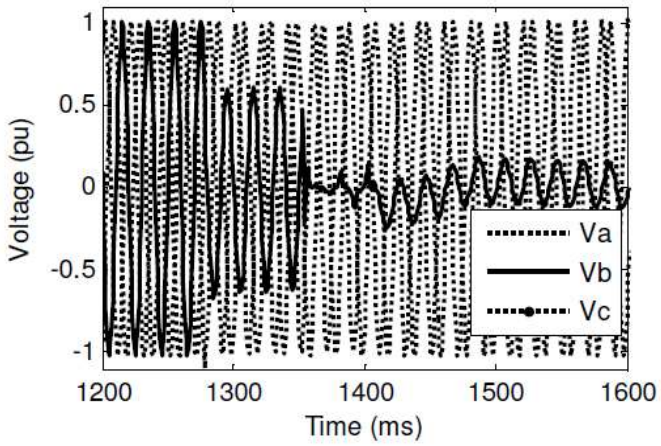

Fig. 15 (a). Three phase voltage at fault instant for Case 1 input waveform

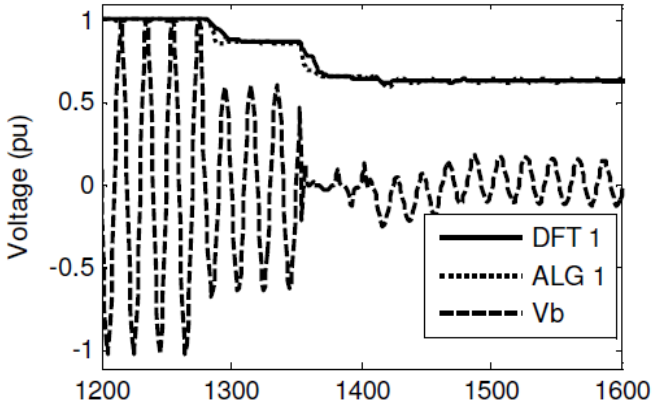

Fig. 15 (b). Positive sequence extraction.

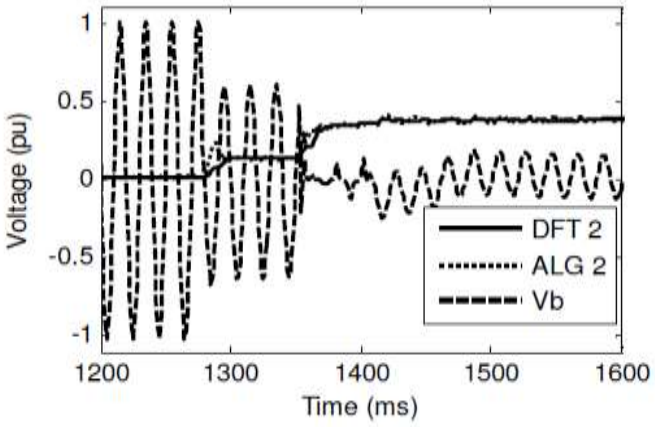

Fig. 15 (c). Negative sequence extraction.

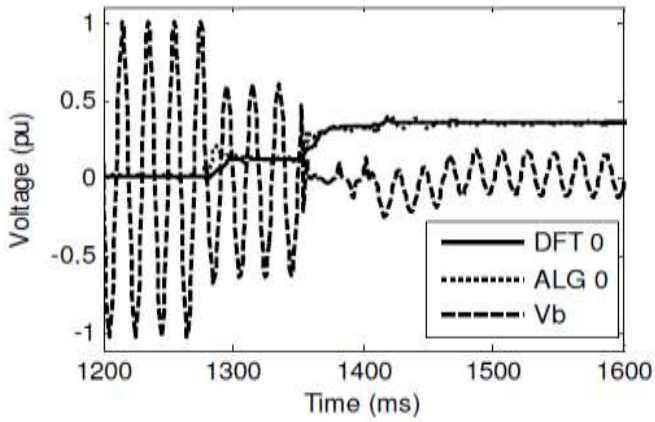

Fig. 15 (d). Zero sequence extraction.

6.2.Case 2

Fault Type 2 is a single line-ground fault on a 275 kV feeder. The source of the fault was a fire. The fault occurred between the Pluto and watershed 275 kV networks.

The sampling frequency was 2.5 kHz. The pre/post-fault voltages are shown in Figure 16 (a). The fault occurred on Phase B at approximately 1.24 seconds. The results indicate that the algorithm model is able to track the symmetrical components of the voltage to within 1% of the DFT on the positive sequence. The algorithm has a steady state error of 3% in relation to that of the DFT on the negative and zero sequence components. The response of the algorithm model, at the inception of the fault, is 10ms for the positive sequence and 6ms for the negative and zero sequence components. This is faster than the response of the DFT. The algorithm responded faster than the DFT with acceptable accuracy for the positive sequence estimation. For the negative and zero sequence estimation, the algorithm responds faster but with less accuracy at the final calculation than the DFT. Figure 16 (a) shows the input waveform with

Figures 16 (b) – (d) showing the comparison of the algorithm and the DFT model for the positive, negative and zero sequence components.

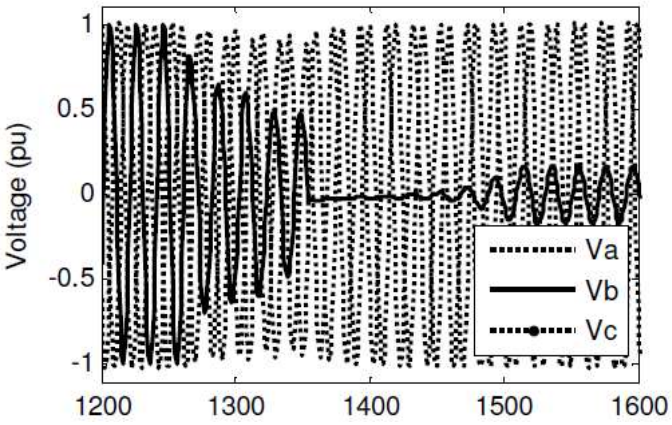

Fig. 16 (a). Three phase voltage at fault instant for Case 1 input waveform

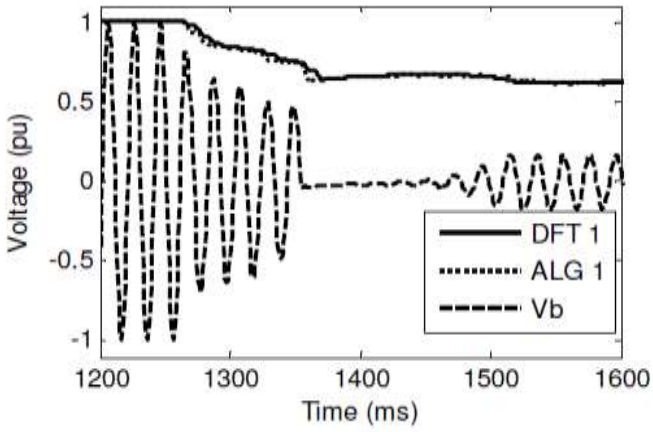

Fig. 16 (b). Positive sequence extraction.

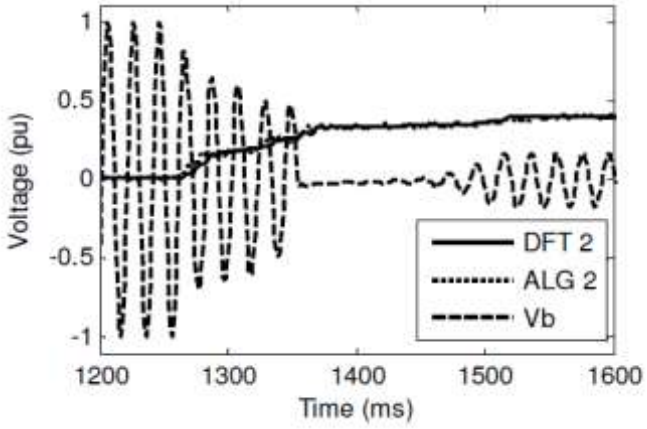

Fig. 16 (c). Negative sequence extraction.

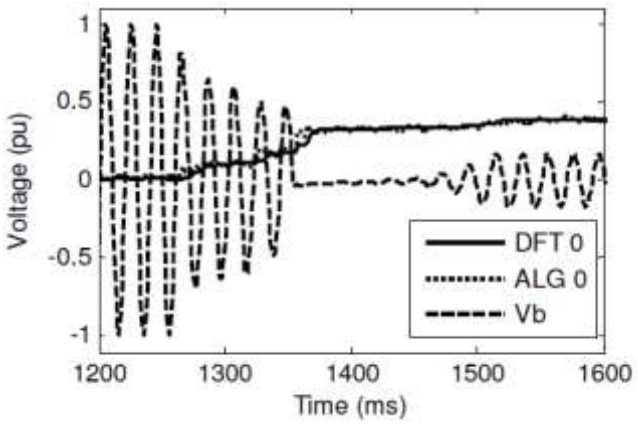

Fig. 16 (d). Zero sequence extraction.

7. *Conclusions*

The results and performance of the proposed method of symmetrical component estimation demonstrate the improvement over the existing DFT method in critical areas. In this paper, a non-linear adaptive method was also presented to estimate symmetrical components in real-time. The method converted a three-phase signal into a time-domain phasor. The standard symmetrical component matrix was used to convert the instantaneous voltage into phasors of the positive, negative and zero sequence components in real-time. The performance of the system under conditions of harmonics and noise was evaluated. The results obtained were benchmarked against theoretical calculations to compare the response of the algorithm and the DFT. The method was experimentally evaluated by injecting actual field voltages into an analog-to-digital processor. The results obtained from the simulation as well as experimental studies confirm the effectiveness of the proposed technique. The proposed method yielded improved response times on most applications. The DFT yielded better accuracy on the negative and zero sequence components of the field data injected.

References

[1] A. M. Stankovic, H. Lev-Ari, and M. M. Perisic, "Analysis and implementation of model-based linear estimation of dynamic phasors," *IEEE Trans. Power Syst*., vol. 19, no. 2, pp. 1903-1910, Nov. 2004.

[2] A. M. Stankovic and T. Aydin, "Analysis of asymmetrical faults in power systems using dynamic phasors," *IEEE Trans. Power Systems*, vol. 15, no. 2, pp. 1062-1068, Aug. 2000.

[3] R. A. Flores, I. Y. H. Gu, and M. H. J. Bollen, "Positive and negative sequence estimation for unbalanced voltage dips," *IEEE Power Engineering Society General Meeting*, vol. 4, pp. 2498-2502, Toronto, Ontario, Canada , July 13-17, 2003.

[4] G. C. Paap, "Symmetrical components in the time domain and their application to power network calculations," *IEEE Trans. Power Systems*, vol. 15, no. 2, pp. 522-528, May 2000.

[5] R. Kumar, B. Singh, and T. Shahani, "Symmetrical components based modified technique for power quality disturbances detection and classification," *IEEE Trans. Industry Applications*, vol. 52, no. 4, pp. 3443 - 3450, Aug. 2016.

[6] C. Fortescue, "Method of symmetrical coordinates applied to the solution of polyphase networks," *Trans. American Institute of Electrical Engineers*, vol. 37, no. 2, pp. 1027-1140, Nov. 1918.

[7] X. Wang, and E. Yaz, "Smart power grid synchronization with fault tolerant nonlinear estimation", *IEEE Trans. Power Systems*, vol. 31, no 6, pp. 4806-4816, Nov. 2016,

[8] H. Darvish, and X. Wang, "Synchronization of unbalanced three phase voltages with nonlinear estimation" *in IEEE Power & Energy Society on Innovative Smart Grid Technologies Conference (ISGT)*, pp. 1-5, Feb. 2015.

[9] D. Yazdani, A., Bakhshai, G. Joos, and M. Mojiri, "A nonlinear adaptive synchronization technique for grid-connected distributed energy sources", *IEEE Trans. Power electronics*, vol. 23, no 4, pp. 2181-2186, Jul. 2008.

[10] R. K. Sinha, and P. Sensarma, "A pre-filter based PLL for three-phase grid connected applications", *Electric Power Systems Research*, vol. 81, no 1, pp. 129-137, 2011.

[11] B. Luna, B. Jacobina, C. Oliveira, and C. Da Silva, "An instantaneous phase angle estimation algorithm for power converters under distorted utility conditions," *Twenty-Sixth Annual IEEE Applied Power Electronics Conference and Exposition (APEC)*, pp. 633-636, 2011.

[12] A. T. Phan, G. Hermann, and P. Wira, "Kalman filtering with a new state-space model for three-phase systems: Application to the identification of symmetrical components," *IEEE International Conference on Evolving and Adaptive Intelligent Systems (EAIS)*, 2015.

[13] D. Duan, X. Zhang, Y. Liu, and D. Xu, "A novel fast detection algorithm for grid symmetrical components extraction," *7th International Power Electronics and Motion Control Conference (IPEMC),* pp. 1998-2001, Jun. 2-5, 2012.

[14] J. L. P. de Sa, "A new Kalman filter approach to digital relaying," *IEEE Trans. Power Delivery*, vol. 7, no. 3, p. 1652-1660, Sept. 1992.

[15] R. Rocha, D. Coury, and R. Monaro, "Recursive and non-recursive algorithms for power system real time phasor estimations", *Electric Power Systems Research*, vol. 143, pp. 802-812, 2017.

[16] I. Arugati, C.M. Orallo, P.G. Donato, S. Maestri, J.L. Strack, and D. Carrica, "Three-phase harmonic and sequence components measurement method based on MSDFT and variable sampling period technique", *IEEE Trans. Instrumentation and Measurement*, vol. 65, no. 8, pp.1761-1772, Aug. 2016.

[17] Y. Kabalci, S. Kockanat, and E. Kabalci, "A modified ABC algorithm approach for power system harmonic estimation problems", *Electric Power Systems Research*, vol. 154, pp. 160-173, 2018.

[18] M. D. Kusljevic, "Symmetrical components estimation through maximum likelihood algorithm and adaptive filtering", *IEEE Trans. Instrumentation and Measurement*, vol. 56, no. 6, Dec. 2007, pp. 2386 – 2394.

[19] V. V. Terzija, D. Markovic, "Symmetrical components estimation through nonrecursive newton-type numerical algorithm", *IEEE Trans. Power Delivery*, vol. 18, no. 2, April 2003, pp. 359 – 363.

[20] R. Naidoo, and P. Pillay, "A new method of voltage sag and swell detection", *IEEE Trans. Power Delivery*, vol. 22, no 2, pp. 1056-1063, 2007.

[21] X. Wang, and E. Yaz, "Smart power grid synchronization with fault tolerant nonlinear estimation," *IEEE Tran. Power Systems*, vol. 31, no. 6, pp. 4806-4816, 2016.

[22] A. K. Ziarani and A. Konrad, "A method of extraction of nonstationary sinusoids," *Signal Processing*, vol. 84, no. 8, pp.1323-1346, 2004.

[23] M. R. Iravani, M. Karimi-Ghartemani, "Online estimation of steady state and instantaneous symmetrical components", *IEE Proc. – Generations, Transmission and Distribution*, vol. 150, Sep. 2003, pp. 616 – 622.